Proc. Estonian Acad. Sci. Phys. Math., 2007, **56**, 2, 207–217

Fatigue characterization of a Cu-based shape memory alloy

Fabio Casciati, Sara Casciati, and Lucia Faravelli

Department of Structural Mechanics, University of Pavia, Via Ferrata 1, 27100 Pavia, Italy; fabio@dipmec.unipv.it

Received 15 January 2007

Abstract. Applications of a Cu-based shape memory alloy in monuments retrofitting were conceived, designed, and tested. The polycrystalline nature of the material requires a preliminary discussion in order to allow the extension of properties which are well known for monocrystalline specimens. Furthermore, one of the main drawbacks of the investigated alloy is its brittleness. Therefore, fatigue tests were carried out and the results of those conducted under cycles of torsion loading–unloading are reported. In particular, the identification of the response range, which is most suitable for structural engineering applications, is pursued.

Key words: compression tests, fatigue tests, shape memory alloy, tension tests, torsion tests, thermal treatment.

1. INTRODUCTION

Shape memory alloys (SMAs) have been the object of theoretical, experimental, and numerical investigations by experts in mathematics [1–3], physics [4–7], metallurgy [8], as well as in engineering sciences [9,10]. As underlined in [11], however, moving from microscale to macroscale often requires beginning the studies from scratch, since the results achieved earlier may be useless.

The next section summarizes the microstructural theory, but also emphasizes the difficulty in generalizing the results of macroscale tests. This is mainly due to the influence of the thermomechanical history of the specimen. Under these premises, the results of macroscale tension/compression tests and torsion tests on the selected Cu-based alloy are illustrated. Finally, the fatigue characterization of the alloy is discussed within the assigned testing conditions.

2. GOVERNING RELATIONS

Microstructural theory [12] is based on the crystallographic and physical knowledge of the material structure and mechanics of deformation. Indeed, it takes account of geometrical and physical peculiarities of the deformation mechanisms. Let us consider a representative volume of the alloy, V, and denote with V_i the volumes of its microregions. The macroscopic deformation tensor ε is obtained by averaging the microdeformation tensors ε_i over all microregions:

$$\varepsilon = \sum_i \frac{V_i}{V} \varepsilon_i = \sum_i \Phi_i \varepsilon_i, \tag{1}$$

where Φ_i is the ith volume fraction. A polycrystal consists of grains characterized by different crystallographic orientations. The orientation of the grains influences most of the properties. Therefore, it is convenient to consider the grains as the volumes of the microregions specified above. Since the grain deformation ε_i' refers to the crystallographic basis, while the macroscopic deformation refers to the laboratory basis, in order to derive the ε_i, some rotation matrices must be introduced in Eq. (1), as is common in continuum mechanics.

Each microregion (i.e. grain) deformation is regarded as the sum of different mechanisms: elasticity, thermal expansion, phase transformation, microplasticity, and plasticity. Let $\varepsilon^{[1]'}_i$, $\varepsilon^{[2]'}_i$, $\varepsilon^{[3]'}_i$, $\varepsilon^{[4]'}_i$, and $\varepsilon_i^{[5]'}$ denote these contributions, respectively. The third and fourth of those require further explanation. If, in the generic ith grain, one observes up to N variants of martensite, the volume fraction of the nth variant is written as Φ_{in}/N. Each martensite variant is characterized by the lattice deformation, D_n, by which it was obtained from the parent phase. It follows that the corresponding phase transformation contribution is given by

$$\varepsilon^{[3]'}_i = \frac{1}{N} \sum_{n=1}^{N} \Phi_{in} D_n. \tag{2}$$

The plastic accommodation is an irreversible deformation occurring in the places of local stress concentrations. Microplastic deformation, geometric incompatibilities, and additional stresses caused by the martensite accommodation remain in the material even after the reverse transformation. This causes the incompleteness of the strain recovery. Here the following expression is postulated for the microplasticity addendum:

$$\varepsilon^{[4]'}_i = \frac{1}{N} \sum_{n=1}^{N} \Phi_{in}^{p} D_n, \tag{3}$$

where Φ_{in}^{p} is the measure of the microstrain produced at the accommodation of the crystal, which belongs to the nth variant of martensite in the grain.

Although the above relationships are difficult to apply at a macroscale level, they show how the material response is affected by the plastic accommodation resulting from both the thermal processes and the stress cycles. Thermal treatments and stress training are therefore introduced to optimize the material predictability.

3. TENSION/COMPRESSION TESTS

The Cu-based alloy which was selected among those available on the market has 11.8 wt% Al and 0.5 wt% Be. It is cast in ingots of 6 kg, from which specimens in the form of wires, bars or plates can be obtained [13–15]. The following phase transformation temperatures were obtained by the differential scanning calorimeter test: martensite starts at −46 °C and finishes at −55 °C; austenite starts at −25 °C and finishes at −18 °C.

Figure 1a provides the stress–strain diagram experimentally obtained from a wire with a diameter of 1 mm. The tension test was conducted in displacement control, without mounting any extensometer, since it requires a larger specimen section. The strains were therefore obtained by dividing the span measurements of the linear variable differential transducer (LVDT), mounted on the testing

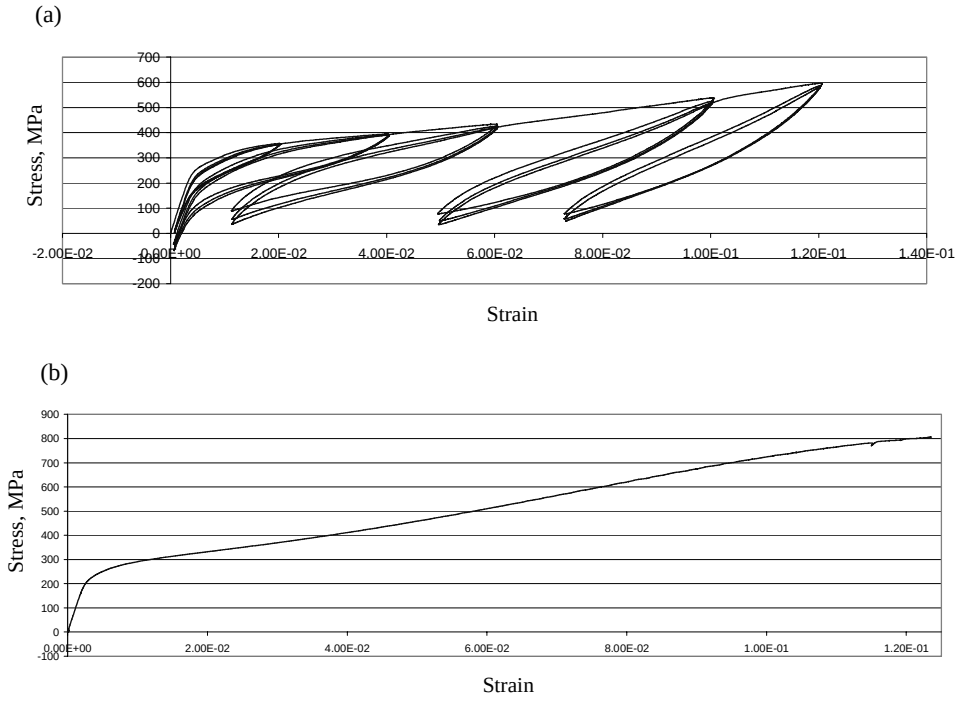

Fig. 1. (a) Loading–unloading cycles on a wire of round section with a diameter of 1 mm: test in displacement control; strain computed by the LVDT. (b) Test to rupture of a wire of round section with a diameter of 3.5 mm: test in displacement control; strain measured by the extensometer.

machine, by the initial length. The comparison with the result (Fig. 1b) of a test to rupture carried out on a wire with a diameter of 3.5 mm of the same alloy (even if coming from a different stock) and mounting the extensometer, shows that the main characters of the alloy are accurately captured in Fig. 1a.

The following remarks arise from Fig. 1:

(a) The virgin curve is abandoned after the first unloading. The higher is the strain reached during the loading, the wider is the gap, which stabilizes after some cycles of the same amplitude.

(b) The first unloading produces small residual strains, which are due to some martensite volume which does not recover into austenite; the residual strain becomes significant when a strain of 5–6% is reached during the loading cycle.

(c) Unloading is badly conducted in displacement control; indeed, at very low values of strain, the residual displacements are associated with negative loads, which theoretically should not be allowed in the wire.

(d) Unloading can be correctly performed in force control, but the machine allows it only for specimens of significant section. Otherwise, the tuning of the testing machine would become a difficult task, often without solution.

It is worth noticing that thermal treatment could be introduced to improve the alloy response in the range of strain up to 4%.

In the following the hollow specimens shown in Fig. 2a will be considered. They were obtained from bars with the external diameter of 15 mm, by removing the internal material to form a pipe with the internal diameter of 12 mm. The results of compression and tension tests at ambient temperature are given in Fig. 3.

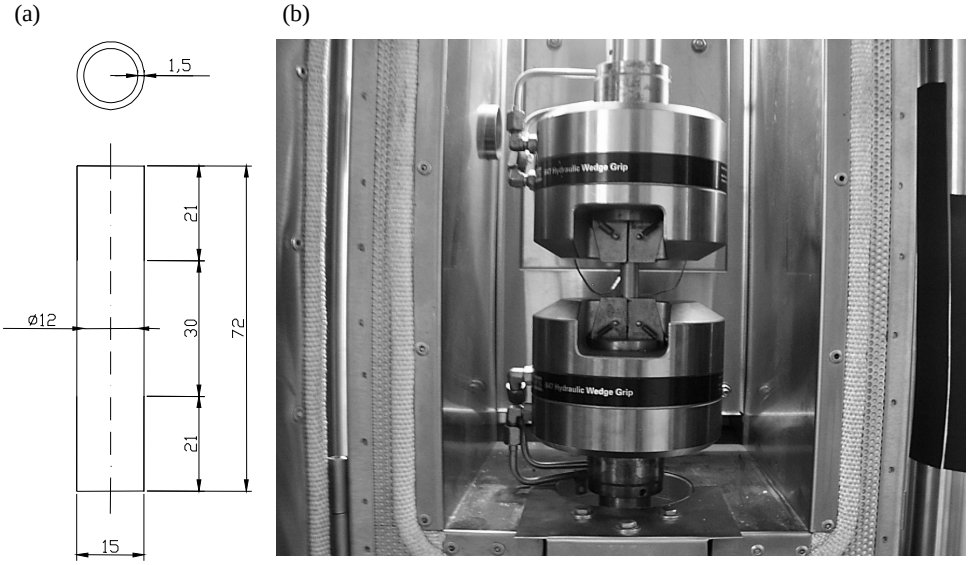

Fig. 2. (a) A SMA specimen for the fatigue test and (b) the testing environments: grips and thermal chamber.

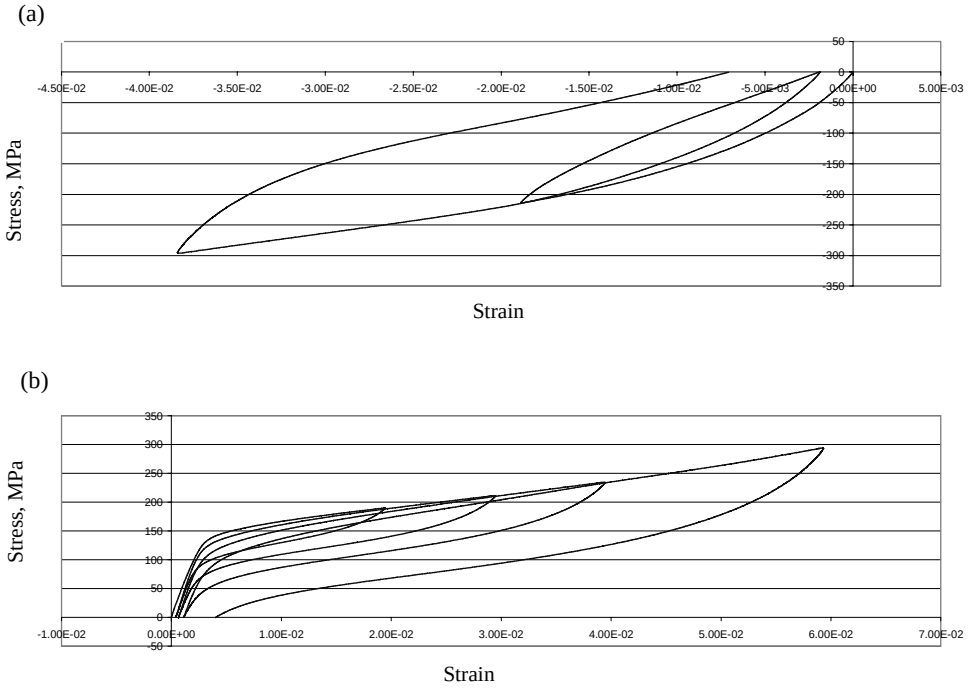

Fig. 3. Stress–strain diagram for the specimen in Fig. 2a: (a) compression test, (b) tension test.

It is worth noting that both the test specifications and the specimen nature are different from those of Fig. 1:

(1) the test is conducted in deformation control during the loading, and in load control during the unloading;

(2) before the test, the specimen undergoes thermal treatment: 4 min at 850 °C, then out at ambient temperature (water quenched), and finally 2 h at 100 °C. The scanning electron microscopy shows re-crystallization and grain growth after thermal treatment. Furthermore, thermal treatment slightly increases the phase transformation temperatures.

From the diagrams of Fig. 3 we can see that

(i) the plateau level has significantly decreased by thermal treatment;

(ii) in tension there is a good recover of strain, even after a loading up to 6% of deformation;

(iii) in compression, un-recovered strains are recorded for any level of peak deformation.

Fatigue tests under tension loading–unloading cycles were discussed in [16,17]. This paper considers only the tests conducted under torsion cycles. The frame-work in which these tests were carried out is clarified in the next section.

4. TORSION TESTS

The universal testing machine in Fig. 2b is bi-axial, i.e., it mounts two hydraulic actuators: axial and torsional. Tests utilizing the latter actuator require specimens of circular section with the external diameter of 15 mm. The ultimate moment of the actuator is 100 N m. In order to reach the material plateau, specimens of hollow circular section and internal diameter of 12.5 mm were used.

The tests were conducted without mounting the torsional extensometer, since its placement requires specimens of a given variable shape (external diameter 15 mm at the top and bottom, but 12.5 mm in the middle). This would have required a too extensive modification transformation of the available alloy pieces.

The specimens underwent several torsion tests driven in angle control. The results of two tests are plotted in Fig. 4: up to rupture (which occurred when the rotation reached 50°; Fig. 4a) and 100 loading–unloading cycles in the range 5°–10° (Fig. 4b).

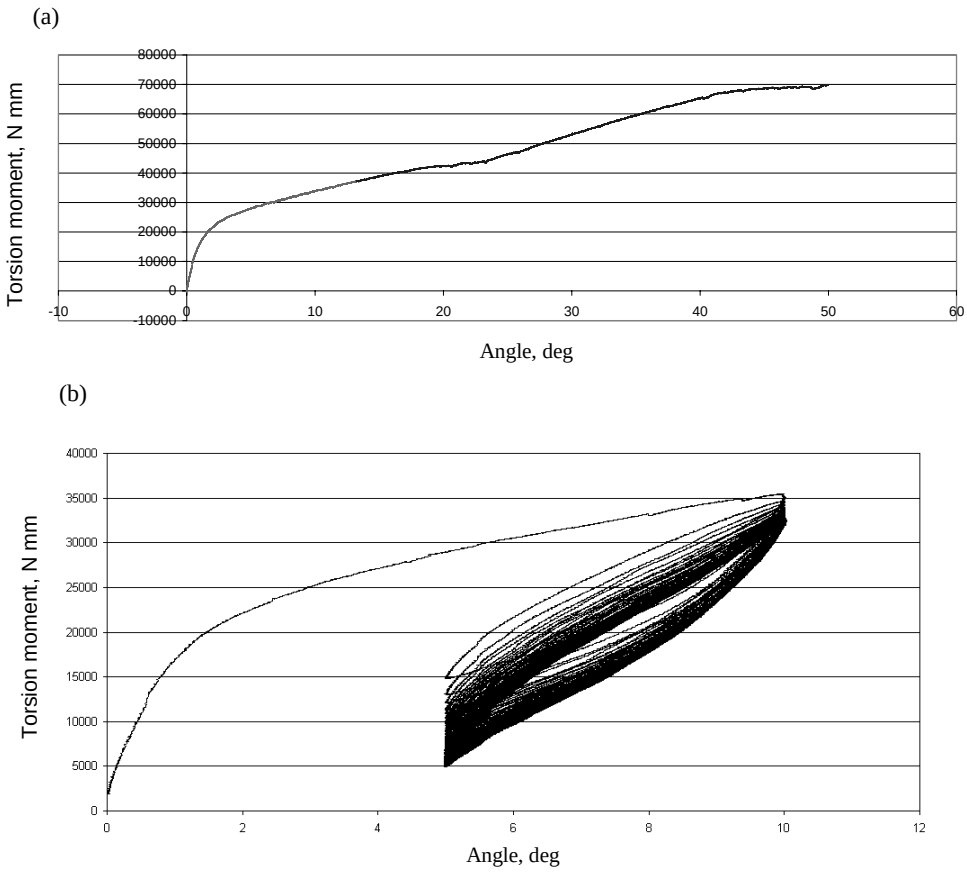

Fig. 4. Torsion moment–angle diagram: (a) up to rupture, (b) 100 cycles in the range 5°–10°.

The main differences from the axial tests discussed in the previous section are the larger internal diameter and the preliminary thermal treatment of the specimen. Here the alloy is left at 100 °C for only 10 min instead of 2 h. This does not satisfactorily prevent the microplasticity effect discussed in section 2. The consequence is evident in Fig. 4b, where each loading–unloading cycle occurs with a loop characterized by a lower value of the residual stress. Since the subject investigated in this paper is the alloy durability, this partial thermal treatment was introduced as a penalty in terms of cycles stabilization, but also as a form of prevention from excessive brittleness.

5. FATIGUE TESTS

Specimens of geometry designed for torsion tests, after the specified thermal treatment, underwent several torsion loading–unloading cycles, each of them entering the stress plateau where austenite transforms into martensite.

Fatigue tests are usually conducted in load control. However, this was not allowed for the alloy under investigation. Indeed,

(a) loading–unloading cycles produce the heating of the specimen; due to the thermoelastic properties of the alloy, this heating requires higher values of the load to be applied in order to reach the plateau;

(b) microplasticity develops along both the principal directions of compression and tension strain direction, thus altering the deformation effect of any given load value.

As a consequence, it was decided to run the tests in angle control, by assigning the peak values at the torsion angle. Then time histories of the maximum torsion moment were recorded (Fig. 5). Two different cases of cycling between two positive values of the peak angles and of cycling around the zero angle are represented in the same figure. They lead to the rupture mechanisms shown in Fig. 6a and 6b, respectively. Both tests were conducted at a frequency of 1 cycle per second.

The angle range is 7.5° for Fig. 5a,b. The observed response, however, is quite different. The maximum moment increases a little in Fig. 5a (mainly due to the heating); after the first material deterioration after 3000 cycles, the specimen survives up to 10 000 cycles. Figure 5b emphasizes a much larger increase in the maximum moment, caused here by the residual strains left during each previous cycle in the opposite direction: a residual strain in compression results in a higher plateau level met in tension, when the rotation sign changes. Moreover, in Fig. 5b the material deterioration is immediately followed by the failure of the specimen, which survives less than 2000 cycles. These different responses were approached in [16] by characterizing each fatigue test by three values of the number of cycles: at the first deterioration, at the point where the curves present a 45° tangent as in Fig. 5, and at the starting point of the final decay. Of course, such an approach makes the two cases in Fig. 5 fully different, since the three triplets are (3000, 10 000, 11 000) and (1700, 1700, 1850), respectively.

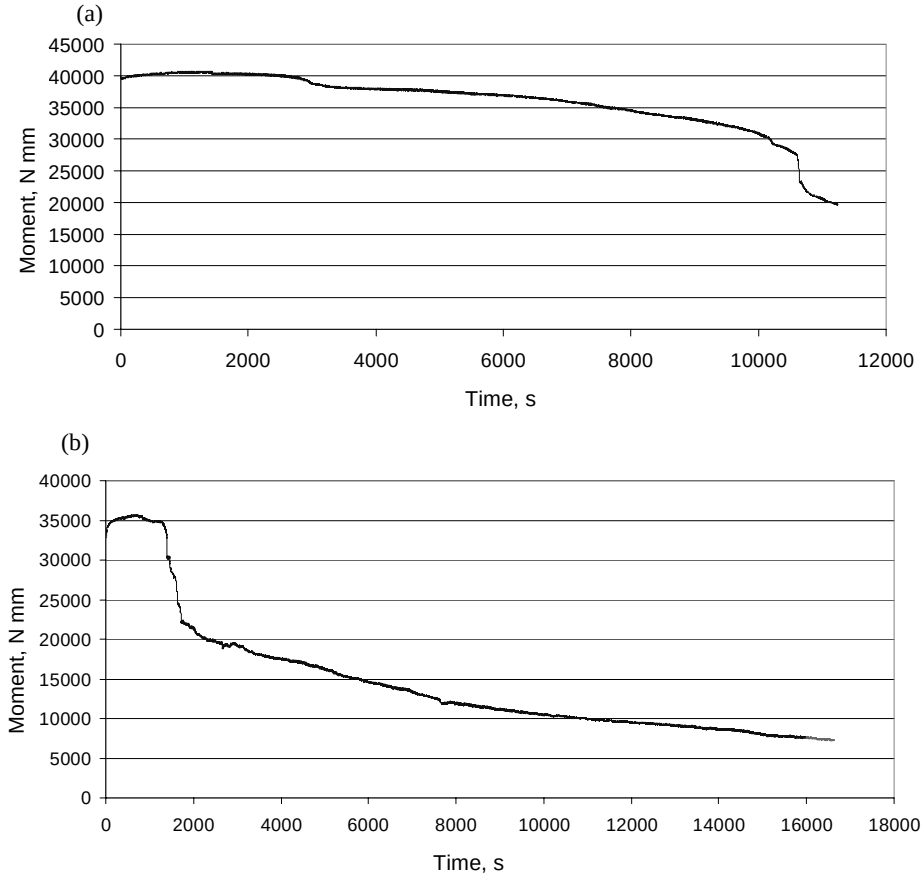

Fig. 5. Evolution of the maximum torsion moment in time: (a) cycles in the range (2.5°, 10°); (b) cycles in the range (–3.5°, 3.5°). Tests conducted at ambient temperature.

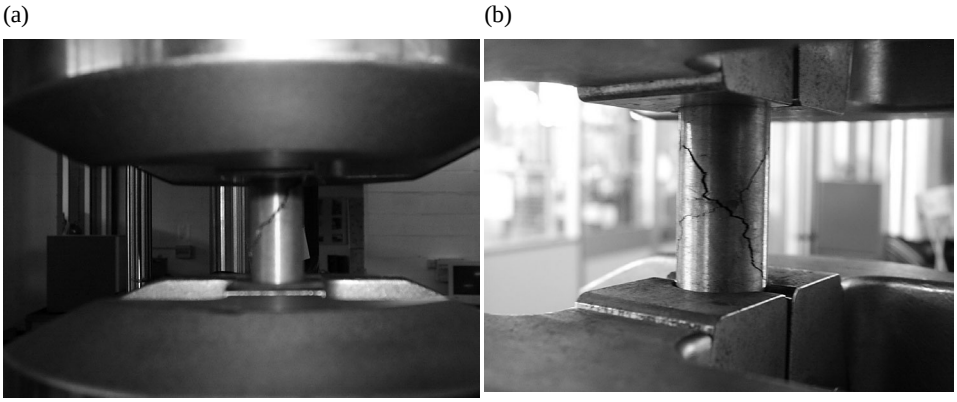

Fig. 6. Mechanism of rupture after fatigue torsion cycles (a) in a positive angle range, (b) around the zero angle.

In order to simplify the presentation of the results, each test is here characterized by the number of cycles after which the maximum torsion moment goes back to the initial value. The results of different tests are summarized in Fig. 7: they were conducted at ambient temperature as well as at 70 °C using the thermal chamber in Fig. 2b. The following observations can be made from Figure 7:

(a) the relationship between the torsion angle and number of cycles to failure can be conveniently interpolated as linear in the case of cycles around zero; a sort of saturation is met for large rotations in the case of cycles between positive peaks;

(b) by increasing the temperature up to 70 °C a significant reduction in the number of cycles to failure is detected; the coefficient of linear regression decreases by one order of magnitude;

(c) in all cases, the alloy is able to survive thousands of cycles, which is reasonably expected in energy dissipation devices during strong winds or earthquakes.

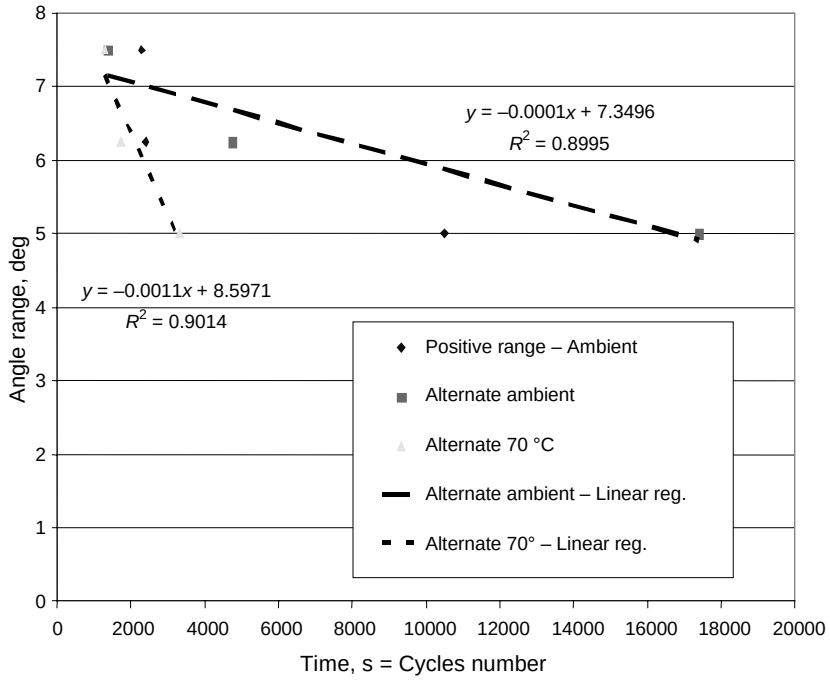

Fig. 7. Angle range of the fatigue test vs. number of survived cycles. Positive ranges start from 2.5°. Alternate tests span from – one half of the angle range to + one half of the angle range.

6. CONCLUSIONS

Pursuing the feasibility of dissipating energy by exploiting the hysteresis cycles of SMA elements requires an investigation of material durability. This study provides some experimental results obtained by performing torsion tests at ambient temperature and at 70 °C. Similar tests which were conducted under cycles of axial loading are reported in [17].

The results of the torsion tests are quite positive in view of the adoption of the studied Cu-based SMA in dissipative devices. A minimum of a few hundreds of survived cycles have to be expected for applications in seismic engineering and a few thousands for application in wind engineering. Both requirements are largely satisfied within reasonable angle ranges. A negative influence of very high temperatures must also be underlined. This requires further tests to be performed to define the allowed temperature range.

A further aspect presently under investigation concerns the influence of the duration of preliminary thermal treatment.

ACKNOWLEDGEMENT

The results summarized in this paper were achieved within the research project WIND-CHIME (Wide-range Non-intrusive Devices toward Conservation of Historical Monuments in the Mediterranean Area) of the 6th Framework Plan of the European Union, for which the first author is serving as coordinator.

REFERENCES

1. Achenbach, M., Atanackovic, T. and Muller, I. A model for memory alloys in plane strain. *Int. J. Solids Struct.*, 1986, **22**, 171–193.
2. Fremond, M. Mécanique des milieux continues. *C. R. Acad. Sci., Série II*, 1987, **304**, 239–244.
3. Patoor, E. and Berveiller, M. *Les Alliages à Memoire de Forme*. Hermès, Paris, 1990.
4. Torra, V. (ed.). *Proceedings COMETT Course: the Science and Technology of Shape Memory Alloys*. University of Balears Islands, Palma de Mallorca, Spain, 1989.
5. Volkov, A., Evard, M., Kurzeneva, L., Likhachev, V. and Sacharov, V. Mathematical modelling of martensitic inelasticity and shape memory effects. *Tech. Phys.*, 1996, **41**, 1084–1101.
6. Leclercq, S. and Lexcellent, C. A general macroscopic description of the thermo-mechanical behavior of shape memory alloys. *J. Mech. Phys. Solids*, 1996, **44**, 953–980.
7. Berezovski, A., Engelbrecht, J. and Maugin, G. A thermoelastic wave propagation in inhomogeneous media. *Arch. Appl. Mech.*, 2000, **70**, 694–706.
8. Funakubo, H. *Shape Memory Alloys*. Gordon and Breach Science Publishers, 1987.
9. Saadat, S., Salichs, J., Noori, M., Hou, Z., Davoodi, H., Bar-on, I., Suzuki, Y. and Masuda, A. An overview of vibration and seismic applications of NiTi shape memory alloy. *Smart Mater. Struct.*, 2002, **11**, 218–229.
10. Casciati, F., Magonette, G. and Marazzi, F. *Technology of Semiactive Devices and Applications in Vibration Mitigation*. John Wiley & Sons, Chichester, UK, 2006.

11. Auricchio, F., Faravelli, L., Magonette, G. and Torra, V. (eds). *Shape Memory Alloys. Advances in Modelling and Applications*. CIMNE, Barcelona, Spain, 2001.
12. Volkov, A. and Casciati, F. Simulation of dislocation and transformation plasticity in shape memory alloy polycrystals. In *Shape Memory Alloys. Advances in Modelling and Applications* (Auricchio, F., Faravelli, L., Magonette, G. and Torra, V., eds). CIMNE, Barcelona, Spain, 2001, 88–104.
13. Casciati, S. and Faravelli, L. Thermo-mechanic characterization of a Cu-based shape memory alloy. In *Proceedings SE04, Osaka, Japan* (Tachibana, E., Spencer, B. F., and Mukai, Y., eds). Bandoh Printing, Osaka, 2004, 377–382.
14. Casciati, F. and Faravelli, L. Experimental characterisation of a Cu-based shape memory alloy toward its exploitation in passive control devices. *J. Phys. IV*, 2004, **115**, 299–306.
15. Casciati, S. and Faravelli, L. Structural components in shape memory alloy for localized energy dissipation. *Comput. Struct.*, 2007 (accepted).
16. Galluzzo, A. *Durabilità di elementi strutturali in lega a memoria di forma*. Master's Degree Thesis, Dept. of Structural Mechanics, University of Pavia, 2006.
17. Casciati, S. and Faravelli, L. Fatigue tests of a Cu-based shape memory alloy. In *Proceedings of 4th World Conference on Structural Control & Monitoring, San Diego, 2006* (to appear).

Vasel (Cu) põhineva kujumäluga sulami väsimuskarakteristikud

Fabio Casciati, Sara Casciati ja Lucia Faravelli

Monumentide restaureerimisel on kasutatud ja katsetatud vasel (Cu) põhinevaid kujumäluga sulameid. Uuringu kaugemaks eesmärgiks ongi nende sulamite omaduste määramine. Monokristallilise proovikeha hästituntud omaduste laiendamine kogu materjalile nõuab täpsemaid uuringuid materjali polükristallilisest olemusest. Näiteks on uuritud sulamite peamiseks puuduseks nende haprus. Artiklis on kirjeldatud väsimuskatseid ja nende tulemusi tsüklilisel väändekoormusel. Eriti on püütud määratleda sulamite sobivaimad rakendusviisid konstruktsioonides.